nature genetics

Cornelia de Lange syndrome is caused by mutations in *NIPBL*, the human homolog of *Drosophila melanogaster Nipped-B*

Ian D Krantz[1], Jennifer McCallum[1], Cheryl DeScipio[1], Maninder Kaur[1], Lynette A Gillis[1], Dinah Yaeger[1], Lori Jukofsky[1], Nora Wasserman[1], Armand Bottani[2], Colleen A Morris[3], Malgorzata J M Nowaczyk[4], Helga Toriello[5], Michael J Bamshad[6], John C Carey[6], Eric Rappaport[1], Shimako Kawauchi[7,8], Arthur D Lander[7], Anne L Calof[7,8], Hui-hua Li[9], Marcella Devoto[9,10] & Laird G Jackson[1,11]

Cornelia de Lange syndrome (CdLS; OMIM 122470) is a dominantly inherited multisystem developmental disorder characterized by growth and cognitive retardation; abnormalities of the upper limbs; gastroesophageal dysfunction; cardiac, ophthalmologic and genitourinary anomalies; hirsutism; and characteristic facial features[1–3]. Genital anomalies, pyloric stenosis, congenital diaphragmatic hernias, cardiac septal defects, hearing loss and autistic and self-injurious tendencies also frequently occur[2]. Prevalence is estimated to be as high as 1 in 10,000 (ref. 4). We carried out genome-wide linkage exclusion analysis in 12 families with CdLS and identified four candidate regions, of which chromosome 5p13.1 gave the highest multipoint lod score of 2.7. This information, together with the previous identification of a child with CdLS with a *de novo* t(5;13)(p13.1;q12.1) translocation, allowed delineation of a 1.1-Mb critical region on chromosome 5 for the gene mutated in CdLS. We identified mutations in one gene in this region, which we named *NIPBL*, in four sporadic and two familial cases of CdLS. We characterized the genomic structure of *NIPBL* and found that it is widely expressed in fetal and adult tissues. The fly homolog of *NIPBL*, Nipped-B, facilitates enhancer-promoter communication and regulates Notch signaling and other developmental pathways in *Drosophila melanogaster*[5].

CdLS is a dominantly inherited disorder with characteristic facial appearance, limb defects (**Fig. 1**) and growth and cognitive retardation. We carried out a genome-wide linkage analysis in nine families with CdLS with more than one affected family member. Under a model of genetic homogeneity, we used a linkage exclusion mapping approach,

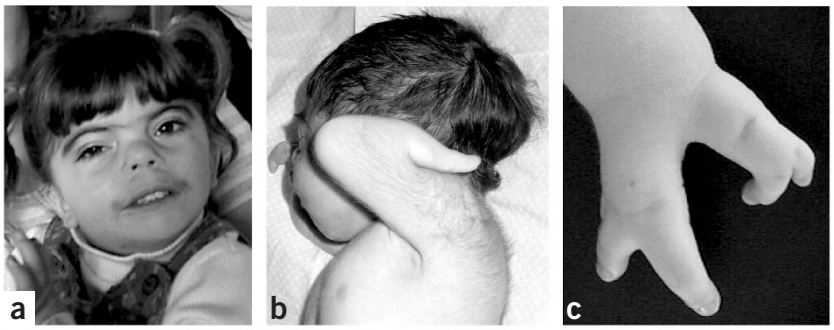

Figure 1 Characteristic features of CdLS. (**a**) Full face view of a child with CdLS showing characteristic facial features, including arched eyebrows with synophrys, long eyelashes, ptosis, depressed nasal bridge with anteverted nares, long philtrum with thin upper lip and micrognathia. (**b**,**c**) Variability of upper limb abnormalities in CdLS. (**b**) Oligodactyly defect with absence of ulna and most digital structures (note also hirsutism of back). (**c**) Distal reduction defect with missing and fused digits.

[1]Division of Human Genetics and Molecular Biology, The Children's Hospital of Philadelphia and The University of Pennsylvania School of Medicine, Philadelphia, Pennsylvania 19104, USA. [2]Division of Medical Genetics, Geneva University Hospital, Geneva, Switzerland. [3]University of Nevada School of Medicine, Las Vegas, Nevada, USA. [4]University Medical Centre, Hamilton, Ontario, Canada. [5]Michigan State University, East Lansing, Michigan, USA. [6]Department of Pediatrics and Department of Human Genetics, University of Utah Health Sciences Center, Utah, USA. [7]Department of Developmental and Cell Biology and [8]Department of Anatomy and Neurobiology, University of California, Irvine, California, USA. [9]Nemours Children's Clinic, Wilmington, Delaware, USA. [10]Department of Oncology, Biology, and Genetics, University of Genoa, Italy. [11]The Division of Obstetrics and Gynecology, Drexel University School of Medicine, Philadelphia, Pennsylvania, USA. Correspondence should be addressed to I.D.K. (ian2@mail.med.upenn.edu).

Published online 16 May 2004; doi:10.1038/ng1364

Table 1 Results of linkage analysis for markers with highest two-point lod scores

Marker	cM	lod score I	II	III	VI	VII	XIII	XIV	XV	XVII	XX	XXI	XXIV	Total lod score 9 families	12 families	Size of linked region (Mb)	Number of of genes
D2S125	260.6	0.30	0.60	0.30	0	–0.03	0.30	0	0.30	0.30	0	0.30	0.18	2.08	2.55	11	160
D5S426	52.0	0	0	0.30	0.30	0.28	0.30	–0.30	0.30	0.30	0	0.18	0	1.49	1.66	14	55
D10S1653	40.4	0	0.60	0.30	0	0.13	0.30	0.18	0.18	0.30	0	0	–0.30	1.98	1.68	21	100
D14S74	87.4	0.30	0.60	0	0.30	0.26	0	0	0.18	0.30	0.18	–0.30	0	1.94	1.82	8	90
D17S938	14.7	0	0.60	0	0.18	0	0.30	0	0	0	0.18	0	–4.40	1.08	–3.14	9	170

Markers were selected from five positive regions after genome-wide scan. The numbers of genes are approximate. Families I–XVII were included in the whole-genome scan. Families XX, XXI and XXIV were typed only for markers that gave positive lod scores in the whole-genome scan.

excluding all markers for which the affected individuals in one or more families did not share both parental alleles (if both parents were unaffected) or the allele transmitted by the affected parent. This analysis identified five regions containing one or more markers with positive lod scores in the nine families (chromosomes 2q37, 5p13, 10p13, 14q24 and 17p13; **Table 1**). We analyzed these five regions in the original nine families and in three additional families with CdLS (total of 12 families) and obtained negative lod scores for *D17S938* in one family, excluding chromosome 17. All other markers gave positive lod scores (**Table 1**).

We carried out fine mapping in all 12 families with additional markers at an average density of 1–1.5 cM in the defined regions on chromosomes 2, 5, 10 and 14. Multipoint linkage analysis did not improve the odds for linkage to chromosomes 2, 10 or 14 but resulted in a maximum lod score of 2.7 for chromosome 5p13, which was the highest score for the entire genome analysis. We refined the critical region on chromosome 5p13 by obligate recombination events to a region of ~7.4 Mb spanning 5p13.1–13.3 flanked by markers *D5S477* distally and *D5S1376* proximally (**Supplementary Fig. 1** online) and containing 58 putative genes (**Fig. 2a**).

We looked for other corroborating evidence to target one or more of the four candidate regions. We previously identified a child with classic features of CdLS and a balanced *de novo* t(5;13)(p13.1;q12.1) translocation, and another child with classic features of CdLS and a *de novo* chromosome 5p13.1–p14.2 deletion (the only reported case of a constitutional deletion of 5p13.2) was recently described[6]. These cases supported the association of 5p13 with CdLS. We next refined the 5p breakpoint in the child with the translocation (samples were not available from the child with the 5p deletion, who died shortly after birth). We carried out fluorescence *in situ* hybridization (FISH) analysis using clones in the minimal critical region on 5p13 of the child with the translocation (**Fig. 2b**). Owing to sample limitations, we could not initially identify a clone that spanned the translocation breakpoint, but

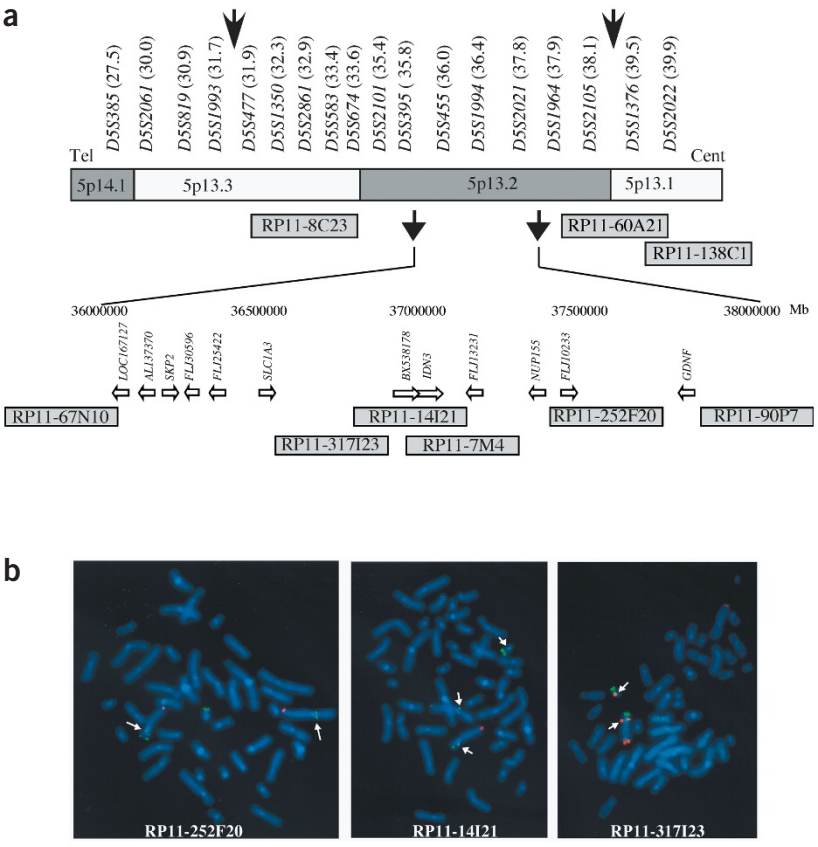

Figure 2 Identification of *NIPBL* as the gene underlying CdLS. (**a**) Critical region on chromosome 5p13, with microsatellite markers and their distances (in Mb) from the p-terminal arm of chromosome 5 indicated above the diagram. Arrows mark the refined critical region after high-resolution analysis and identification of obligate recombination events. BAC clones used for FISH analysis are indicated by their RP11 addresses. FISH analysis further narrowed the critical region, as shown by arrows below the diagram. The expanded view identifies genes in the defined critical region (from the July 2003 build of the University of California Santa Cruz genome browser). (**b**) FISH analysis using BACs from the linkage-defined chromosome 5p13 critical region. The chromosome 5p telomeric control probe is labeled in green and the 5q telomeric control probe is labeled in red. In the left panel, BAC RP11-252F20 is labeled in green. Both signals from BAC RP11-252F20 are on chromosome 5 p (arrows), indicating that it is proximal to the translocation breakpoint. In the middle panel, BAC RP11-14I21, which contains *NIPBL*, is labeled in green. There is signal on both of the chromosome 5p arms as well as on chromosome 13q (arrows), indicating that the probe was split on the translocated chromosome. In the right panel, BAC RP11-317I23 is labeled in red. One signal is present on the normal chromosome 5p arm and the other is present on 13q, indicating that this probe is distal to the translocation breakpoint.

Table 2 Mutations and clinical features in individuals with CdLS

Mutation	Exon	Effect	Clinical features
2G→A (M1K)	2	Altered start codon	Family II: mutation identified in all three affected siblings (who each have a different father) but was not present in their mother or in the two fathers from whom samples were available. All three siblings (an 8-year-old girl and 17-year-old and 3-year-old boys) have moderate growth and cognitive delays, small hands without reduction defects, hirsutism and typical facial features.
150delG	3	Stop codon 28 amino acids downstream	Male child seen at 4.5 months of age with severe bilateral upper limb reduction defects (oligodactyly, single digit), severe growth and cognitive delays, typical facial features, hirsutism and a cleft palate.
1546–1547insG	10	Stop codon 3 amino acids downstream	Female adult seen at 23 years of age with severe growth and cognitive delays, reduction defect of the right limb (oligodactyly, four digits) and small left hand with no reduction defect, typical facial features, hirsutism, cleft palate and hearing loss.
2520delT	10	Stop codon 5 amino acids downstream	Male child seen at 3.5 years of age with severe growth and cognitive delays, small hands with no reduction defects, typical facial features, hirsutism, undescended testes and bilateral sensorineural hearing loss.
3023–3027delTGTCT	10	Stop codon 1 amino acid downstream	Female child seen at 10 years of age with severe growth and cognitive delays severe bilateral upper limb reduction defects (oligodactyly, single digit), hirsutism and typical facial features.
6735+5 G→T	39	Splice site disruption	Family XXI: mutation identified in the two affected siblings but neither parent. The two siblings, a 6-year-old boy and a 5-year-old girl, both have growth and cognitive delays, small hands without reduction defects, typical facial features and hirsutism.

we narrowed the critical region to an interval of 1.1 Mb containing 11 putative genes (**Fig. 2a**).

We carried out mutational analysis of the first three exons of all 11 genes by conformation-sensitive gel electrophoresis (CSGE)[7] and identified mutations in two overlapping transcripts, *BX538178* (3,653-bp mRNA) and *IDN3* (8,124-bp mRNA; **Fig. 2a**). The identification of mutations in both transcripts (in *BX538178*-specific sequence, in *IDN3*-specific sequence and in the overlap region) and their exact sequence identity over a 2,259-bp region of overlap suggested that they were part of a larger transcript, which we called *NIPBL* (Nipped-B like). CSGE analysis of the complete coding sequence of *NIPBL* in 30 probands (including the 12 familial probands) identified mutations in 2 familial and 4 sporadic cases of CdLS (20% mutation detection rate; **Table 2** and **Supplementary Fig. 2** online). In three of the four sporadic cases for which samples from both parents were available, the mutations were *de novo*. In one sporadic case (3023-3027delTGTCT), samples were available from only the mother, and she did not carry the mutation. All four mutations identified in sporadic cases were frameshift mutations (three deletions and one insertion). The two familial mutations (a missense mutation in family II in the first codon (2G→A, causing the amino acid substitution M1K) and a splice site mutation in family XXI (6763+5G→T) in intron 39) were identified in all affected siblings and were not present in any of the parents, implicating germline mosaicism as a mechanism in familial recurrences where neither parent manifests features of the disorder.

All mutations are expected to result in a truncated or, in the case of the M1K mutation, untranslated protein. The mutations are spread throughout the gene and were not seen in 300 normal ethnically matched control chromosomes. We identified seven sequence polymorphisms (**Supplementary Table 1** online).

We studied expression patterns by northern-blot and *in situ* analyses. Northern blots of fetal and adult samples for multiple probes detected transcripts of ~6 kb and 1.9 kb transcripts and, in fetal samples, additional bands of ~9.5 kb and 7.2 kb (**Supplementary Fig. 3** online). The presence of multiple transcripts is suggestive of alternative splicing for this gene. Transcripts of the mouse homolog of *NIPBL* were detected widely at gestation days 9.5 and 10.5 (**Fig. 3**), with notable accumulations in limb bud, branchial arch and craniofacial mesenchyme. These regions are involved in patterning of the skeleton and soft tissues of the limbs, jaw and face (among others).

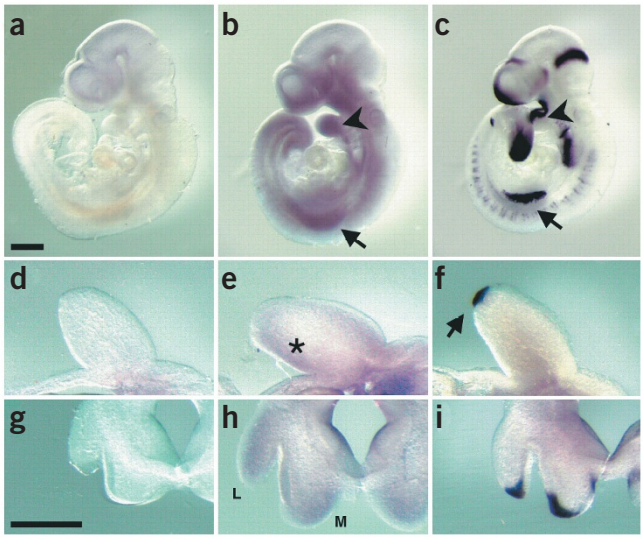

Figure 3 Expression of *NIPBL* in the developing mouse. (**a**–**c**) Embryonic day (E) 9.5 embryos, whole-mount *in situ* hybridization. (**d–i**) E10.5 embryos, vibratome sections (200 m) of embryos processed for whole-mount *in situ* hybridization. (**a**,**d**,**g**) Sense control. (**b**,**e**,**h**) Mouse homolog of *NIPBL*. (**c**,**f**,**i**) *Fgf8* (positive control). (**b**) The mouse homolog of *NIPBL* is expressed throughout the embryo, especially in the limb buds and branchial arches (arrow, fore limb bud; arrowhead, first branchial arch). (**c**) *Fgf8* expression marks a portion of the surface ectoderm of the same structures (arrow and arrowhead as in **b**). (**e**,**f**) At E10.5, sections through the forelimb bud show that expression of the mouse homolog of *NIPBL* is concentrated in the mesenchyme (asterisk in **e** marks ventral limb bud mesenchyme; dorsal mesenchyme is also stained), whereas *Fgf8* expression marks the apical ectodermal ridge (arrow in **f**). No significant differences in intensity between fore- and hindlimb buds were observed (data not shown). Coronal sections at the level of the head show expression of the mouse homolog of *NIPBL* in the mesenchyme of both the lateral (L) and medial (M) nasal processes (**h**). In contrast, *Fgf8* hybridization marks the ectoderm surrounding the developing nasal pit. Scale bars: **a**, 0.5 mm (for **a–c**); **g**, 0.5 mm (for **d–i**).

We amplified cDNA isolated from lymphoblastoid cell lines, compared it with sequences in the University of California Santa Cruz and National Center for Biotechnology Information genomic databases and determined that *NIPBL* is represented by two overlapping transcripts: *BX538178* (3,653-bp mRNA) and *IDN3* (8,124-bp mRNA). We confirmed this by northern-blot analyses using probes generated from sequence-specific regions of these two transcripts. The genomic sequence spans 188 kb, and the mRNA is 9,505 bp (coding region, bases 127–8,539), encoding a protein of 2,804 amino acids. The mRNA comprises 47 exons, with one 5′ noncoding exon. The protein sequence of human NIPBL shares 92% identity with mouse, 88% with rat and 37% with the fruit fly *Nipped-B* gene product (SIM alignment). In a BLAST search of the National Center for Biotechnology Information database, NIPBL also had substantial homology with the *Saccharomyces cerevisiae* sister chromatid cohesion protein 2, which forms a complex with SCC4 and is required for the association of the cohesin complex with chromosomes[8]. We used the PROSITE program to search for conserved motifs and found that NIPBL has a bipartite nuclear targeting sequence (amino acids 1,108–1,124) and a putative HEAT repeat. HEAT repeats (originally identified in the huntingtin protein) are found in condensins, cohesins and other complexes with chromosome-related functions[9].

Nipped-B is an essential regulator of *cut*, *Ultrabithorax* and Notch receptor signaling. Its protein product belongs to the family of chromosomal adherins, and genetic evidence suggests that it has an architectural role in facilitating long-distance interactions between enhancers and promoters[5]. The involvement of Nipped-B in regulating Notch signaling is of interest, as two other genes involved in Notch signaling are implicated in human developmental disorders (mutations in *JAG1* result in Alagille syndrome[10], and mutations in *DLL3* result in spondylocostal dysostosis[11]).

The identification of mutations in a single allele of *NIPBL* in individuals with CdLS is consistent with a dominant pattern of inheritance. All mutations identified so far predict a truncated protein product and probably result in functional haploinsufficiency. That haploinsufficiency is a mechanism in CdLS is confirmed by the child with a large deletion of the region (encompassing *NIPBL*) and severe manifestations of CdLS[6], and by the child with the translocation reported here, who also has severe manifestations.

In this report we show that mutations in *NIPBL* cause CdLS. Because the paucity of familial cases and consistent cytogenetic rearrangements did not allow for standard positional cloning approaches, we identified this gene by combining information on candidate regions not excluded by linkage analysis with other supporting data (cytogenetic rearrangements). The expression pattern of *NIPBL*, and the mechanism of action suggested by its structural homologs, provides insight into the pathogenesis of the defects seen in the multiple systems involved in CdLS.

METHODS

Individuals with CdLS. We verified that all affected individuals enrolled in the study were diagnosed with CdLS. All affected individuals and unaffected family members were enrolled in the study under a protocol of informed consent approved by the Institutional Review Board at The Children's Hospital of Philadelphia.

Genome-wide linkage analysis. We carried out linkage studies using the ABI linkage mapping set version 2, consisting of 400 fluorescently labeled polymorphic markers spaced at intervals of ~10 cM throughout the genome. We estimated marker allele frequencies used in the lod score analysis based on alleles observed in the families' founders. We carried out model-based two-point and multipoint linkage analysis on data from the whole-genome scan and from the fine mapping of chromosomes 2, 5, 10 and 14 in all families using the GENEHUNTER computer program version 2.0 (ref. 12). For lod score analysis, we assumed the disease to follow an autosomal dominant mode of inheritance with disease allele frequency of 0.00001. To account for the possibility that the disease in families with unaffected parents was due to germline mosaicism in one of the parents, we coded all unaffected individuals (parents and siblings) from whom samples were available for genotyping as unknown at the disease phenotype. Thus, we did not have to assume anything about the unknown penetrance of the putative mutation underlying CdLS. We retained marker genotype information from unaffected siblings when such information was available and used it to reconstruct phase for haplotyping. Marker maps used in multipoint linkage analysis were sex-averaged genetic maps from the Center for Medical Genetics of the Marshfield Clinic Research Foundation.

FISH. We carried out FISH analysis using standard techniques as described previously[13]. We used BAC clones to the critical region on chromosome 5p13.2 (from telomere to centromere: RP11-8C23, RP11-67N10, RP11-317I21 (AC026463.5), RP11-14I21, RP11-7M4, RP11-252F20, RP11-90P7, RP11-60A21 and RP11-138C1) identified through the University of California Santa Cruz genome browser as probes to refine the position of the chromosome 5p13 breakpoint of the t(5;13)(p13.1;q12.1) translocation. We obtained the BACs from Children's Hospital of Oakland Research Institute. We extracted total BAC DNA (Perfectprep Plasmid XL, Eppendorf Scientific) and labeled it with spectrum orange or green dUTP by nick translation using a commercially available kit (Vysis). We combined labeled DNA with Cot-1 DNA. We carried out hybridization and washes using standard conditions.

Mutational analysis and CSGE. We carried out CSGE according to standard protocols[7]. Oligonucleotide primer sequences and PCR conditions used for amplification of all exons of the *NIPBL* are available on request. We purified PCR products corresponding to all altered migration patterns (shifts) using QIAquick PCR purification kit (QIAGEN Sciences) and sequenced them on an ABI 377 sequencer.

Northern-blot analysis. We hybridized poly(A)$^+$ RNA northern blots of multiple adult human tissues (Human 12-Lane Multiple Tissue Northern (MTN) Blot BD Biosciences Clontech) and human fetal tissues (MessageMap Northern Blot, Stratagene) with a 301-bp probe from *BX538178*-specific cDNA sequence (*NIPBL* exon 2 and 3), a 344-bp probe from *IDN3*-specific cDNA sequence (*NIPBL* exon 46 and 47) and a 252-bp probe from a region of overlap between the two putative transcripts (*NIPBL* exon 10; all primer sequences available on request). We used the BD SpotLight Random Primer Labeling Kit (BD Bioscience Clontech) to label probes and SpotLight Chemiluminescent Hybridization & Detection Kit (BD Bioscience Clontech) for hybridization and visualization. Experiments were duplicated using Ready-to-go DNA labeling beads (- dCTP; Amersham) with ^{32}P-dCTP and purified on ProbeQuant G-50 microcolumns (Amersham). We blocked blots with yeast tRNA and herring sperm DNA. We visualized the signal by exposure to autoradiograph film for 1–5 min (chemiluminescent) and 1–4 h (^{32}P).

***In situ* hybridization.** We generated a probe for the mouse homolog of *NIPBL* by PCR from an EST clone (oligonucleotide primer sequences available on request), which yielded a 389-bp product corresponding to the last 190 bp of exon 10 and all of exon 11 of human *NIPBL* (Table 2). We subcloned this fragment into pCRII-TOPO (Invitrogen) to generate antisense and sense digoxigenin-labeled cRNA probes. We generated an *Fgf8* probe (positive control) from a 422-bp *Nco*I-*Pst*I fragment of the *Fgf8* cDNA (bp 59–481 of GenBank Z48746) cloned into pBluescript. We dissected CD-1 (Charles River) mouse embryos at days 9.5 and 10.5 of gestation and fixed and processed them for whole-mount *in situ* hybridization, with detection using alkaline phosphatase–conjugated sheep antibodies to digoxigenin and 5-bromo-4-chloro-3-indolyl phosphate/nitroblue tetrazolium as the chromagenic substrate[14].

URLs. The University of California Santa Cruz genome browser is available at http://genome.ucsc.edu/cgi-bin/hgGateway. The National Center for Biotechnology Information genome database is available at http://www.ncbi.nlm.nih.gov/. The PROSITE program is available at http://us.expasy.org/cgi-bin/scanprosite. SIM alignment is available at http://us.expasy.org/cgi-bin/sim.pl. The Center for Medical Genetics of the Marshfield Research Foundation is available at http://research.marshfieldclinic.org/genetics/.

Accession numbers. GenBank: Human *IDN3*, NM_133433; mouse *IDN3* homolog BG070859 and XM_127929; rat *IDN3* homolog, XM_238213; *NIPBL*, BK005151. GenBank protein: *Saccharomyces cerevisiae* sister chromatid cohesion protein 2, Q04002.

Note: Supplementary information is available on the Nature Genetics website.

ACKNOWLEDGMENTS

We thank the individuals with CdLS and their families for their support and willingness to donate samples; the Cornelia de Lange Syndrome Foundation, their staff and their director J. Mairano for their support; and N. Spinner, M. Jackson, A. Kline, J. Morrissette, M. Budarf and the staff of the clinical cytogenetics laboratory and the sequencing core at The Children's Hospital of Philadelphia for their comments and guidance. This work was supported by grants from the National Institutes of Health, National Institute of Child Health and Human Development (to I.D.K., M.D., A.D.L. and A.L.C.).

COMPETING INTERESTS STATEMENT

The authors declare that they have no competing financial interests.

Received 27 January; accepted 31 March 2004
Published online at http://www.nature.com/naturegenetics/

1. de Lange, C. Sur un type nouveau de dégénératio (typus Amstelodamensis). *Arch. Méd. Enfants* **36**, 713–719 (1933).
2. Jackson, L., Kline, A.D., Barr, M.A. & Koch, S. de Lange syndrome: a clinical review of 310 individuals. *Am. J. Med. Genet.* **47**, 940–946 (1993).
3. Ireland, M., Donnai, D. & Burn, J. Brachmann-de Lange syndrome. Delineation of the clinical phenotype. *Am. J. Med. Genet.* **47**, 959–964 (1993).
4. Opitz, J.M. The Brachmann-de Lange syndrome. *Am. J. Med. Genet.* **22**, 89–102 (1985).
5. Rollins, R.A., Morcillo, P. & Dorsett, D. Nipped-B, a Drosophila homologue of chromosomal adherins, participates in activation by remote enhancers in the cut and Ultrabithorax genes. *Genetics* **152**, 577–593 (1999).
6. Hulinsky, R. *et al*. Prenatal diagnosis dilemma: fetus with del(5)(p13.1p14.2) diagnosed postnatally with Cornelia de Lange syndrome. *Am. J. Hum. Genet.* **73** Suppl., 602 (2003).
7. Ganguly, A., Rock, M.J. & Prockop, D.J. Conformation-sensitive gel electrophoresis for rapid detection of single-base differences in double-stranded PCR products and DNA fragments: evidence for solvent-induced bends in DNA heteroduplexes. *Proc. Natl. Acad. Sci. USA* **90**, 10325–10329 (1993).
8. Ciosk, R. *et al*. Cohesin's binding to chromosomes depends on a separate complex consisting of Scc2 and Scc4 proteins. *Mol. Cell* **5**, 243–254 (2000).
9. Neuwald, A.F. & Hirano, T. HEAT repeats associated with condensins, cohesins, and other complexes involved in chromosome-related functions. *Genome Res.* **10**, 1445–1452 (2000).
10. Li, L. *et al*. Alagille syndrome is caused by mutations in human Jagged1, which encodes a ligand for Notch1. *Nat. Genet.* **16**, 243–251 (1997).
11. Bulman, M.P. *et al*. Mutations in the human delta homologue, DLL3, cause axial skeletal defects in spondylocostal dysostosis. *Nat. Genet.* **24**, 438–441 (2000).
12. Kruglyak, L., Daly, M.J., Reeve-Daly, M.P. & Lander, E.S. Parametric and nonparametric linkage analysis: a unified multipoint approach. *Am. J. Hum. Genet.* **58**, 1347–1363 (1996).
13. Krantz, I.D. *et al*. Deletions of 20p12 in Alagille syndrome: frequency and molecular characterization. *Am. J. Med. Genet.* **70**, 80–86 (1997).
14. Kawauchi, S. *et al*. Regulation of lens fiber cell differentiation by transcription factor c-Maf. *J. Biol. Chem.* **274**, 19254–19260 (1999).